Detection of Burst Noise using the Chi-Squared Goodness of Fit Test

by

Shubra Marwaha, B.S.E.E

Report

Presented to the Faculty of the Graduate School of

The University of Texas at Austin

in Partial Fulfillment

of the Requirements

for the Degree of

Master of Science in Engineering

The University of Texas at Austin

August, 2009

Detection of Burst Noise using the Chi Squared Goodness of Fit Test

Approved by
Supervising Committee:

Arjang Hassibi

Eric Swanson

Abstract

Detection of Burst Noise using the Chi Squared Goodness of Fit test

Shubra Marwaha, M.S.E

The University of Texas at Austin, 2009

Supervisor: Arjang Hassibi

Statistically more test samples obtained from a single chip would give a better picture of the various noise processes present. Increasing the number of samples while testing one chip would however lead to an increase in the testing time, decreasing the overall throughput. The aim of this report is to investigate the detection of non-Gaussian noise (burst noise) in a random set of data with a small number of samples.

In order to determine whether a given set of noise samples has non-Gaussian noise processes present, a Chi-Squared 'Goodness of Fit' test on a modeled set of random data is presented. A discussion of test methodologies using a single test measurement pass as well as two passes is presented from the obtained simulation results.

Table of Contents

List of Figures

List of Tables

Chapter 1: Introduction

Almost all experimental signals have noise components present due to random fluctuations of observable physical quantities. Noise in electronic circuits is usually regarded as detrimental as it imposes a practical limit on the performance of the circuit. The Dynamic Range is a measure of the ratio of the largest signal and the lowest signal that can be processed in a circuit. The lowest signal in a circuit is primarily set by the noise level.

On occasion, noise inherent in a circuit can be exploited. Examples of this include the intentional addition of thermal noise in some Analog to Digital Converters used to improve the Dynamic Range by dithering. Noise inherent in a circuit could also be exploited as a means of investigating the electrical characteristics of the circuit [1].

1.1: THERMAL AND BURST NOISE

The most common and well understood form of noise present in all chips is thermal noise. Thermal noise arises due to random charge carrier fluctuations in resistive materials.

Burst noise on the other hand, is an uncommon form of noise. It was first observed in early point contact diodes and during the commercialization of one of the first semiconductor op-amps [2]. Current circuit technologies have greatly reduced the number of units affected by burst noise but on occasion units with low levels of burst noise can still be identified. Burst noise is detrimental in audio circuits as the distinct "popping" sound characteristic of low frequency burst noise can be easily delineated.

Thermal noise levels in most audio applications are reduced to levels inaudible by the human ear.

1.2: MOTIVATION

Noise measurements are typically set up to collect output time samples from a chip under specified input conditions. The time samples can be analyzed using statistical tests as well as through a frequency spectrum obtained from the Discrete Fourier Transform (DFT). References [3] and [4] highlight some of the common statistical and frequency tests used in noise measurements of Analog to Digital Converters.

Statistically more test samples obtained while testing one chip would make it easier to identify low levels of burst noise. This however leads to an increase in the test time, decreasing the overall throughput.

A primary target of this study is to construct a test methodology that increases the percentage of units detected with burst noise with a low sample size/test time. For the purpose of this study, bad parts are defined as parts with both thermal and burst noise while good parts are defined as parts with only thermal noise. Another principal specification aimed for in this study is a 99% yield (% good parts passed) and detection of 95% of parts with burst noise (% bad parts failed).

In order to achieve this target, a Chi-Squared 'Goodness of Fit' test on a modeled set of random data with burst and thermal noise is explored. The Goodness of fit test is used to determine whether a given set of noise samples has contributions from burst noise processes.

1.3: OUTLINE

Chapters 2 and 3 provide a brief background on the Chi-Squared Distribution and the Discrete Fourier Transform (DFT) used as part of the test. Characteristics of the thermal and burst noise modeled in this study are discussed in Chapter 4. The Chi-Squared Goodness of Fit test and possible test flows that are derived from the simulation studies are highlighted in Chapters 5-7.

Chapter 2: Chi Squared Distribution

The probability density function of a the Chi-Squared distribution (χ^2) is defined as

$$f(x) = \frac{1}{2^{k/2}\Gamma(v/2)} x^{(v/2)-1} e^{-x/2} \quad , \; x > 0 \qquad 2.1$$

where v is the degrees of freedom and Γ is the gamma function:

$$\Gamma(r) = \int_0^\infty x^{r-1} e^{-x} \, dx \text{ for r} > 0 \qquad 2.2$$

The mean and variance of the χ^2 distribution are v and 2v respectively. The chi-squared distribution is non-negative and has a positive skew. As the degrees of freedom increase the distribution becomes more symmetric and with $v \to \infty$, it approaches the normal distribution [5]. Chi-squared distributions for varying degrees of freedom are shown in Fig 2.1.

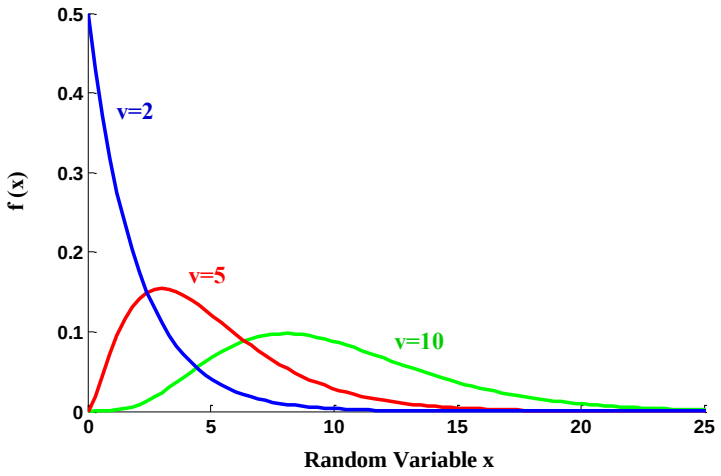

Figure 2.1: Chi-Squared Distribution with varying degrees of freedom (v).

2.1: CHI-SQUARED PERCENT POINT

The percentage points or value of the chi-square random variable ($\chi^2(\alpha,v)$) with v degrees of freedom is defined as

$$P(X^2 > \chi^2(\alpha,v)) = \int_{\chi^2(\alpha,v)}^{\infty} f(u)\, du = \alpha \qquad 2.3$$

This is shown as the shaded region in Fig 2.2.

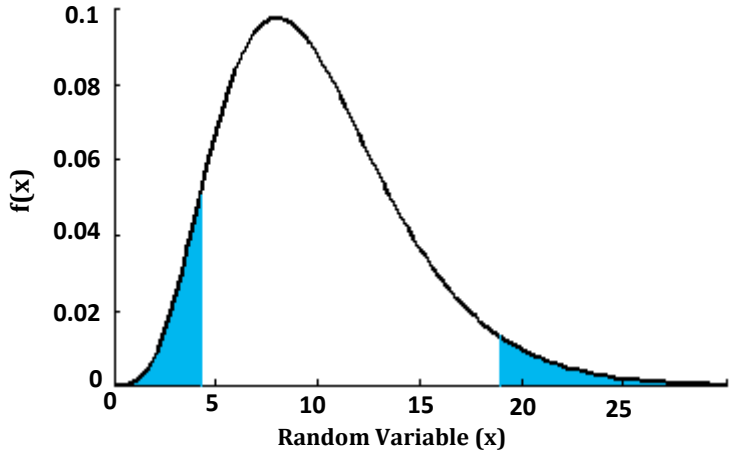

Figure 2.2: Chi-Squared Distribution with v =10.

Fig 2.2 plots the chi-squared distribution for 10 degrees of freedom. The total area under the Chi Squared Distribution is normalized to one. As shown in the plot, the value with v = 10 and α (right shaded area) = 0.05 is $\chi^2(0.05,10)$ =18.31. This value is also expressed as the upper 5% point with 10 degrees of freedom. Conversely, a lower 5% point with 10 degrees of freedom (left shaded area) would be $\chi^2(0.95,10)$ =3.94 [5]. The chi-squared percent point in this study are obtained from the in-built chi2inv(p,v) Matlab function [6]. Chi-Squared statistics are extensively used in the estimation of variance, independence tests and tests of distributions.

Chapter 3: Discrete Fourier Transform

The Discrete Fourier Transform (DFT) corresponds to equally spaced frequency samples of the Fourier transform of a signal [7]. The DFT of a set of N time samples (a_0,a_1,a_2….,a_{N-1}) is a set of N frequency bin values (A_0,A_1,A_2,….,A_{N-1}) derived using:

$$A_m = \sum_{n=0}^{N-1} a_n W_N^{mn} \tag{3.1}$$

where $W_N = e^{-j\frac{2\pi}{N}}$ and m =0,1,…N-1.

As DFT deals with samples and bins with no concept of frequency, for each sample spaced at interval T, the bin m can be related to frequency by:

$$f = \frac{m * f_S}{N} \tag{3.2}$$

where $f_S = \frac{1}{T}$ is the sampling frequency. The total time spent gathering time samples is the reciprocal of the DFT resolution and can be calculated as $t = N * T$.

The Discrete Fourier Transform is periodic with period N and sampled data frequency response repeats every f_S (which corresponds to m = N) with the magnitude response symmetric around $f_S/2$ [8]. This is as bin values above fs/2 (m > N/2) are complex conjugates of values below fs/2 (m < N/2):

$$A_{N-m} = \sum_{n=0}^{N-1} a_n W_N^{(N-m)n} = \sum_{n=0}^{N-1} a_n W_N^{nN} W_N^{-mn} = \sum_{n=0}^{N-1} a_n W_N^{nN} = A_m^* \tag{3.3}$$

$$W_N^{Nn} = e^{-j\frac{2\pi(Nm)}{N}} = 1.$$

For most purposes, the frequency response is only plotted till $f_S/2$ with 0 corresponding to the DC bin and $f_S/2$ corresponding to 'Daylight'.

The bin values A_m obtained from the DFT of real time samples are usually complex with exception of the dc bin (m=0) and the fs/2 bin (m=N/2) [8].

$$A_M = B_M + jC_M \tag{3.4}$$

$$A_0 = \sum_{n=0}^{N-1} a_n \tag{3.5}$$

$$A_{N/2} = \sum_{n=0}^{N-1} a_n e^{-j\pi n} = \sum_{n=0}^{N-1} a_n (-1)^n \tag{3.6}$$

3.1 ENERGY THEOREM

The Energy theorem of the DFT requires that all the energy in the time domain must show up in the frequency domain scaled by 1/N,

$$\sum_{n=0}^{N-1} |\, a_n \,| = \frac{1}{N} \sum_{m=0}^{N-1} |\, A_m \,|^2 \tag{3.7}$$

This can be written in terms of root mean square values as:

$$\sqrt{\frac{1}{N} \sum_{n=0}^{N-1} |\, a_n \,|^2} = \sqrt{\frac{1}{N^2} \sum_{m=0}^{N-1} |\, A_m \,|^2}$$

$$a_{rms} = \frac{1}{N} \sqrt{\sum_{n=0}^{N-1} |\, A_m \,|^2} \tag{3.8}$$

3.2 DFT MAGNITUDE PLOTS

DFT magnitude plots are plotted on a log scale and normalized with respect to a full scale sine wave with root mean squared value a_{FS} (dBFS scale). A full scale sine

wave input would yield a peak bin value of 0dbFS. The equation below highlights the normalization used:

$$|A_m|(dBFS) = 20\log_{10}\frac{|A_m|}{Na_{FS}/\sqrt{2}} \qquad 3.9$$

Figure 3.1 shows a DFT magnitude plot on a dBFS scale from dc to $f_S/2$ of a 1Vrms, 100 kHz sine wave sampled at 1MHz [8].

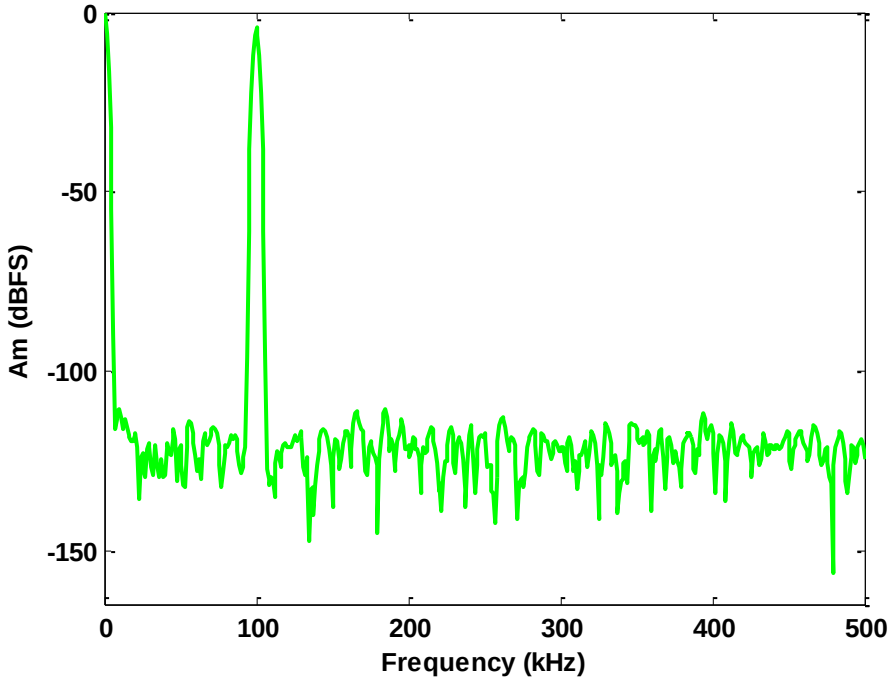

Figure 3.1: 1000 point DFT, 1Vrms full-scale, 100 kHz sine wave.

Chapter 4: Noise

Electrical noise comprises any unwanted random electrical signals that are added to desired signals in a circuit. Noise can be attributed to the physical noise sources intrinsic to devices in a circuit (mainly due to the discrete nature of charge), as well as to the noise generated by circuit operation [9]. The minimum signal level that can be detected and processed with acceptable quality is limited by the amount of noise in a circuit.

The common forms of physical noise sources encountered in circuits are: Thermal noise, Flicker noise (1/f noise), Shot noise and Burst noise. As this study primarily investigates thermal and burst noise, these noise processes are described in detail in the sections below.

4.1: THERMAL NOISE

Thermal noise is a fundamental physical phenomenon, present in any passive resistor above absolute zero temperature. It arises from the random velocity fluctuations of charge carriers in a resistive material occurring regardless of any applied voltage [1]. The amplitude distribution of thermal noise is Gaussian.

Thermal noise has flat power spectral density as it is uniformly distributed over all frequencies. As a result, resistor rms noise voltage in a 10Hz band centered at 1 kHz is the same as resistor rms noise in a 10Hz band centered at 1GHz [8].

Thermal noise in resistors has a voltage squared value given by:-

$$e^2 = 4kTRB \qquad 4.1$$

where k = Boltzmann's Constant , R = resistance in ohms, T = Absolute temperature in K and B = measurement bandwidth in Hz. Resistor noise spectral density N_0 is the root mean square (rms) noise per √Hz in bandwidth B and can be expressed as:

$$N_0 = \sqrt{\frac{e^2}{B}} = \sqrt{4kTR} \qquad 4.2$$

N_0 for a 1kΩ resistance at room temperature is 4nV/√Hz.

4.2: BURST NOISE

Burst noise appears as random set changes of offset voltage, with two or more discrete levels, that take place at variable intervals in time. It can also be viewed as a square wave with random changeovers onto which other noise components (thermal, flicker, shot) are superimposed [9]. The amplitude distribution of burst noise is Non-Gaussian.

Authors in Ref. 9 indicate the source of burst noise in semiconductors is the imperfect nature of the semiconductor's crystal structure. It primarily occurs in MOSFETs' due to the trapping of carriers by active traps in the oxide, or by scattering centers in the vicinity of the inversion layer of the device.

The power spectrum of burst noise is essentially flat at low frequencies with a $1/f^2$ roll-off at high frequencies [1]. In the equation below f_C represents the corner frequency of the burst noise.

$$S(f) = \frac{P}{1+\left(\frac{f}{f_C}\right)^2} \qquad 4.3$$

Burst noise is also known in literature as Random Telegraph Signal (RTS) noise and Popcorn noise (named due to the "popping" sound heard when played through an audio system).

4.3: THERMAL AND BURST NOISE

In a system with both thermal and burst noise present, the noise spectral density in a bandwidth from f to frequency f+df is given by:

$$e^2(f)df = 4kTR_{EQ}\left[1+\left(\frac{f_C}{f}\right)^2\right] \qquad 4.4$$

The first term in the equation is the thermal noise term and the second is the burst noise term [8]. At the burst noise corner frequency, the thermal noise and burst noise contributions to the total noise spectral density are equal. Below the corner frequency the total noise spectral density is dominated by the burst noise while beyond the corner frequency the spectral density is dominated by the thermal noise. This is highlighted in Figure 4.1.

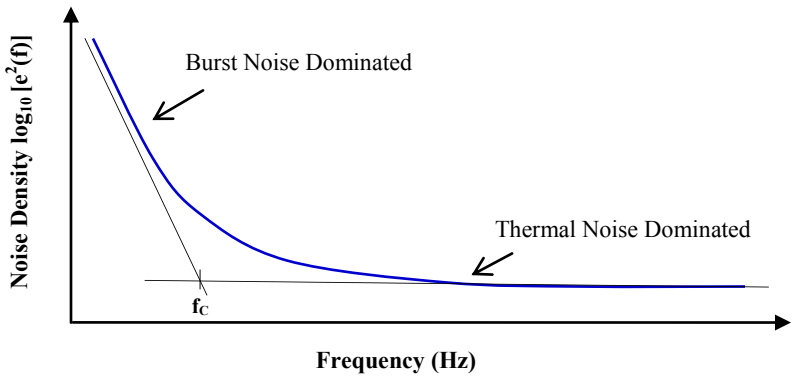

Figure 4.1: Total Noise Density (log) vs. Frequency

4.4: THERMAL AND BURST NOISE MODELS

Thermal Noise Model:

The thermal noise time domain model is generated using the in-built Matlab randn(m) function, which generates m normally distributed pseudo-random numbers with a specified mean and standard deviation [6]. For this study, the thermal noise samples are generated with a standard deviation of 30μVrms. Figure 4.2 shows the modeled thermal noise.

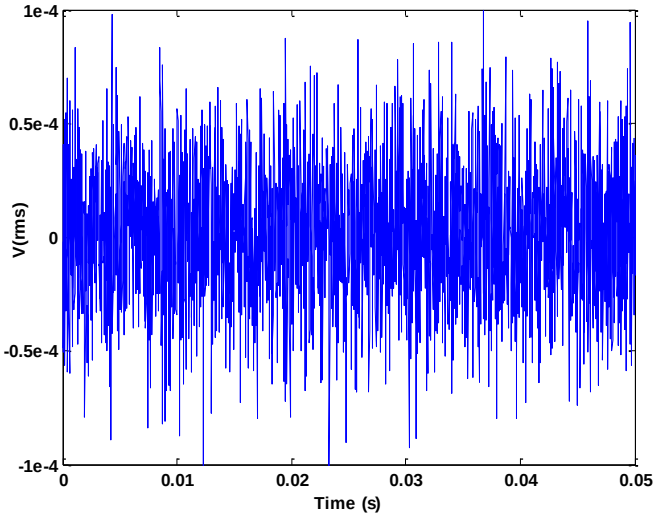

Figure 4.2: Thermal noise (Vrms) vs. time(s)

Burst Noise Model:

As burst noise is characterized by a random period, uniform random numbers between -0.5 and 0.5 (generated using the Matlab rand(z) function) are used to determine the time period. The generated uniform random numbers (n) are quantized using the signum function (sign(n) function in Matlab) which scales n to 1 if $n > 0$ and to -1 if $n < 0$ [6]. Thermal noise is then added to the quantized spectrum and the total spectrum

generated is scaled in order to generate a burst noise spectrum with 10μV amplitude. The Matlab code used to generate the noise models is included in the Appendix.

Figure 4.3 below shows the generated burst noise time domain model.

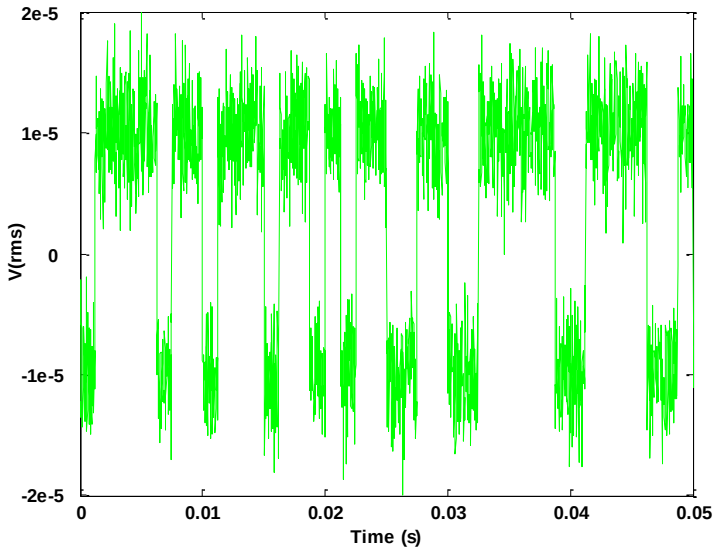

Figure 4.3: Burst noise (Vrms) vs. Time(s)

Chapter 5: Pearson's Chi – Squared Goodness of Fit Test

The Chi-Squared Goodness of Fit Test was first investigated by Karl Pearson. It is used to determine whether a given set of data with an unknown distribution belongs to a hypothesized distribution. The test procedure requires random samples of size n from an unknown distribution which is arranged into a frequency histogram with k bins [10]. This is used to generate the test statistic defined as:

$$X^2 = \sum_{i=1}^{k} \frac{(O_i - E_i)^2}{E_i} \qquad 5.1$$

where O_i is the frequency in the i^{th} bin of the unknown distribution. E_i is the count frequency generated from the hypothesized probability distribution.

5.1: Use of the Goodness of Fit test to detect Burst Noise

The aim of this study is to correctly fail bad parts with both burst and thermal noise and pass good parts which only have thermal noise. As burst noise is non-Gaussian, binned test data is compared against frequency counts generated using a Gaussian distribution (E_i).

Burst noise when added to thermal noise makes the noise distribution Non-Gaussian. Figure 5.1 highlights the change in the distribution when decreasing levels of burst noise are added to thermal noise. The red trace in Fig 5.1 is generated with both thermal and burst noise while the blue trace is generated with only thermal noise. With the burst noise rms voltage twice that of the thermal noise (Figure 5.1 (a)), the total distribution can be clearly identified as Non-Gaussian. With the burst noise rms voltage a third of the thermal noise (Figure 5.1 (d)), the presence of the burst noise is not clearly visible.

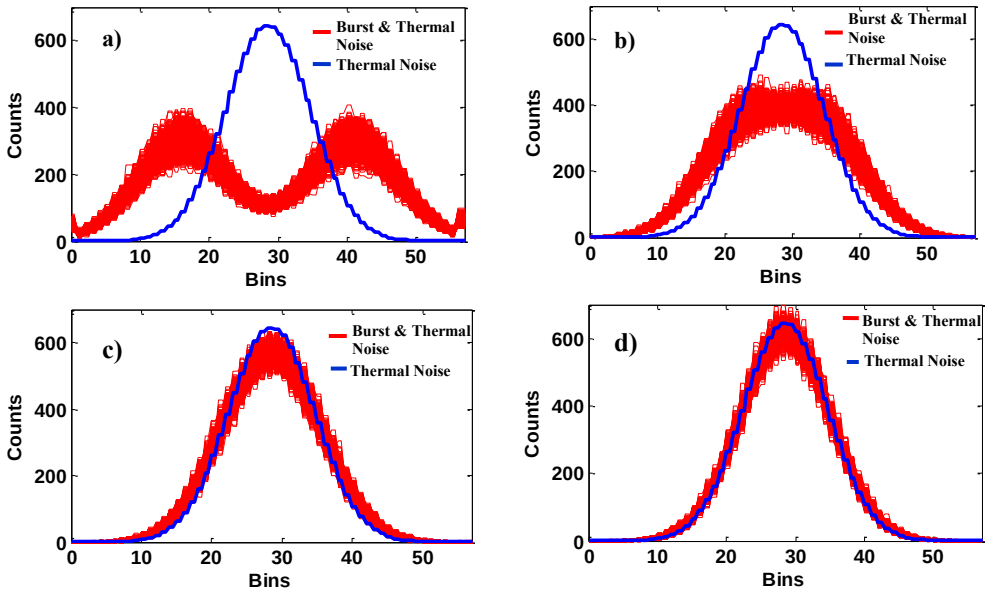

Figure 5.1: 30µVrms thermal noise with:- (a) 60µVrms burst noise. (b) 30µVrms burst noise (c) 15µVrms burst noise and (d) 10µVrms burst noise

5.2: COMPARISON OF TEST STATISTIC

In-order to determine the validity of the test, the test statistic generated (X^2) is compared with $\chi^2(\alpha,v)$, where $\chi^2(\alpha,v)$ is the theoretical chi squared percent point value. $\chi^2(\alpha,v)$ is determined by two parameters:- v, the degrees of freedom and α, the statistical significance [5]. These parameters are discussed in detail in the section below.

The test data is determined as Gaussian, if $X^2 < \chi^2(\alpha,v)$ indicating a part will pass the test. Alternatively if $X^2 > \chi^2(\alpha,v)$, the test data is not Gaussian and the part fails the test. This is summarized in the Table 5.1 below.

Outcome	Conclusion
$X^2 < \chi^2(\alpha,v)$	**Unknown Distribution is Gaussian. Part Passes the Test.**
$X^2 > \chi^2(\alpha,v)$	**Unknown Distribution is not Gaussian Part Fails the Test**

Table 5.1: Test Outcomes

5.3: STATISTICAL TERMS

Statistical Significance (α):

The statistical significance indicates the probability that the test will fail a good part. In other words, if a set of known good parts are tested with α set to 0.1, 10% of the parts would fail the test. Failing a good part would result in a Type I error which is set by the α value.

Degrees of Freedom (v):

The degrees of freedom are the number of independent comparisons that are made in order to calculate the test statistic (X^2) [6]. Theoretically the degrees of freedom are equal to the no of bins (k)-1. However every parameter that is estimated causes a loss of a degree of freedom. The corrected degrees of freedom is equal to v = k-p-1, where p is the number of estimated parameters. As the mean and variance are estimated in this test, p is set to two.

Power of the Test (β):

The power of the test (β) is probability that the test fail a bad part. It depends on both the sample size and α. A larger sample size makes it easier to detect a bad part while using of lower values of α increases the power of the test. Passing a bad part results in a Type II error (1-β). This is summarized in Table 5.2.

Results	Good Part	Bad Part
Pass	No error	Type II error (1-β)
Fail	Type I error (α)	No error

Table 5.2: Summary of Type I and II errors

5.4: EXPECTED GAUSSIAN COUNTS (E_I)

The Expected Gaussian Counts (E_i) are generated from the theoretical cumulative density function (cdf). The cdf (F(x)) is the probability that a random variable X takes a value less than or equal to x [1]:

$$F(x) = \Pr[X \le x] \qquad 5.2$$

The probability that a random variable X takes a value between x_1 and x_2 can therefore be obtained as:

$$\Pr[x_1 \le X \le x_2] = F(x_2) - F(x_1) \qquad 5.3$$

The Gaussian cdf for zero mean and standard deviation σ is illustrated in Fig 5.2.

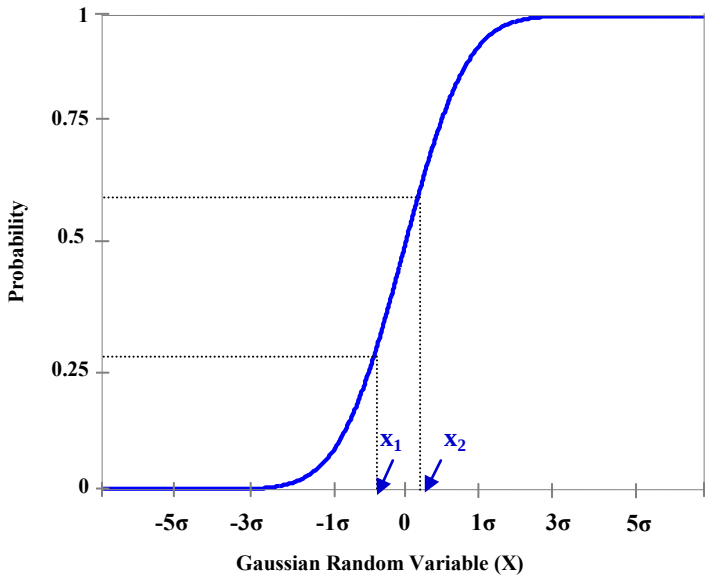

Figure 5.2: Gaussian CDF with zero mean and standard deviation σ.

If the cdf is divided into k bin intervals , $x_1, x_2, x_3 \ldots, x_k$, the expected Gaussian counts can be calculated as:

$$E_i = n\sum_{i=0}^{k}\left[F(x_{i+1}) - F(x_i)\right] \qquad 5.4$$

where n is the total sample size [11].

In order to use the theoretical Gaussian cdf, the mean and variance are estimated using the methods discussed below.

Estimation of Mean and Variance

Mean :

The mean ($\overline{X}$) of the Observed Data is estimated using the expression:

$$\overline{X} = \frac{1}{n}\sum_{i=1}^{n} X_i \qquad 5.5$$

where n is the total number of samples and X_i is the i^{th} random variable.

Variance:

Method 1:

Beyond the corner frequency of the burst noise, the relative magnitude of the burst noise is small as compared to the thermal noise. As a result the frequency spectrum is dominated by the response of the thermal noise at higher frequencies.

The variance of the thermal noise is estimated by taking the Discrete Fourier Transform (DFT) of the observed data. From the DFT magnitude response, the variance is estimated by summing the noise power in bins from $f_S/4$ (m=n/4) to $3f_S/4$ (m = 3n/4). In order to extend the variance estimate from DC to Daylight, the noise power in these bins is doubled. The equation below shows the expression used to determine the thermal noise variance:

$$\sigma^2 = \frac{1}{N^2}\left[2\sum_{m=\frac{n}{4}}^{\frac{3n}{4}-1} |A_m|^2\right] = \frac{1}{N^2}\left[2\sum_{m=\frac{n}{4}}^{\frac{3n}{4}-1} \left\langle B_m{}^2 + C_m{}^2 \right\rangle\right] \qquad 5.6$$

where $A_m = B_m + jC_m$ is the m^{th} frequency bin value. The bins used in this calculation are highlighted in Fig 5.3 below.

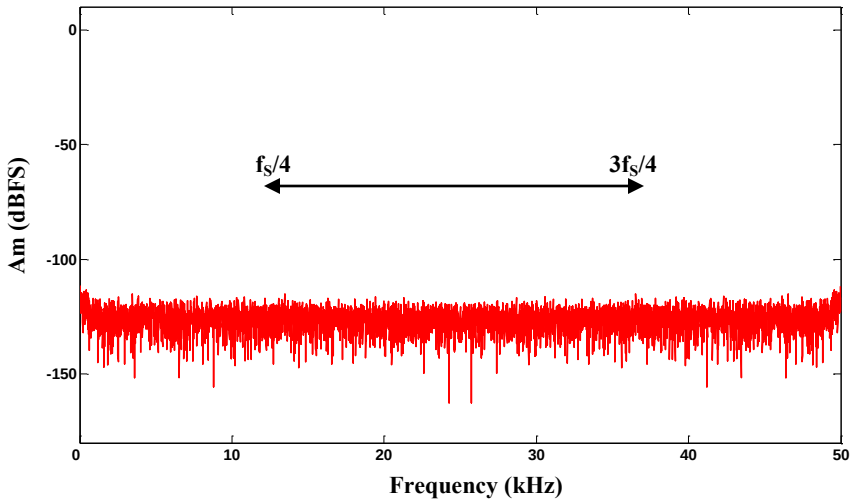

Figure 5.3: DFT Magnitude Response (Thermal and Burst noise) vs. Frequency (f_s =50 kHz)

Method 2

As an alternative method, the variance of the observed data was estimated using:

$$\sigma^2 = \frac{1}{n}\sum_{i=1}^{n}(X_i - \overline{X}) \qquad 5.7$$

The estimate for the variance described in Method 1 allowed the test to fail a larger percent of parts with burst noise as compared to the estimate from Method 2. Therefore the estimate in Method 1 is used to generate the expected counts.

5.5: CHOICE OF BINS

The bin intervals needed in order to generate both the Expected and Observed counts are derived from the Expected Distribution. If the expected count frequency within a bin is too small, the test will not accurately reflect the departure of observed frequencies from the expected [10]. The bin intervals are therefore chosen in order to ensure each bin has a minimum of 5 counts.

The bin intervals can be determined using equiprobable bins as well as bin widths specified by Sturges' Formula. There was not a significant difference between results obtained using both methods but as the equiprobable binning method allows a fixed bin size, it was used to generate the final results. The bins are partitioned from 3σ to -3σ.

Equi-probable Bins

Bins are created using the Gaussian cdf with an equal probability in each bin interval. This will ensure that all the expected bins E_i have the same count frequency. Figure 5.4 illustrates the frequency of counts with equiprobable bins.

Empirical studies have suggested that equal probable bin boundaries provide an unbiased test and a more accurate approximation to the chi squared distribution [10].

Sturges' Formula

Binning of the test data can also be done using Sturges' Formula [12] where z is the bin width and n is the total number of samples. This method however provides varying bin sizes (k) as the total number of samples (n) is varied.

$$z = \log_2 n + 1 \qquad 5.8$$

The count frequencies illustrated in Fig 5.1 were created using bin widths calculated using Sturges' formula.

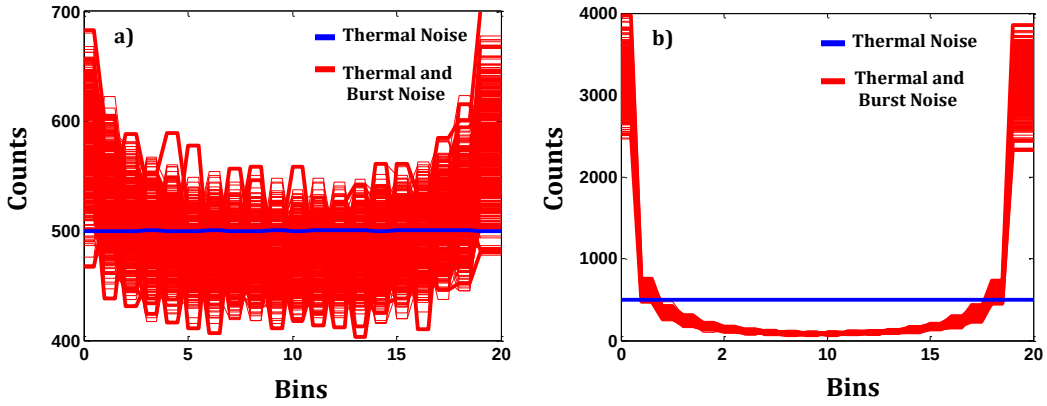

Figure 5.4: (a) 10μVrms burst noise and 30μVrms thermal noise (b) 60μVrms burst noise and 30μVrms thermal noise with equiprobable binning.

Bin Size

Previous simulation studies [10] show that standard statistics with fewer bins result in a better power. An optimum bin size suggested by Mann and Wald is:

$$M = 1.88n^{\frac{2}{5}} \qquad 5.9$$

where n is the sample size.

Chapter 6: Simulation Results

Results were obtained by simulating 10000 known good parts (parts with only thermal noise) and 10000 known bad parts (parts with both thermal and burst noise) using the Chi Squared Goodness of fit test. The following sections highlight the test methodology and results obtained.

6.1: PARTS SIMULATED

Good Parts

Good parts were simulated by generating Gaussian time samples using the in-built Matlab function, randn(n), in-order to model data from a part with only thermal noise. The root mean square (rms) value of the thermal noise was scaled to ensure that within a 0-20kHz bandwidth; the total integrated noise was about -90dBVrms. The rms value was thus set at 30μVrms.

Bad Parts

Bad parts were modeled by adding time samples from the burst noise model (discussed in Chapter 4) to the generated thermal noise samples.

The burst noise power was kept as a tenth of the noise power of the thermal noise. The rms value of the burst noise was thus a third of the thermal noise rms value and set at 10μVrms.

Figure 6.1 provides the time domain samples generated in-order to obtain the results of this study. The addition of burst noise with an rms value at a tenth of the thermal noise does not provide any significant visible change in the total time domain waveform. This is highlighted in Figure 6.1(c). Figure 6.2 shows the DFT magnitude response of the thermal and burst noise samples.

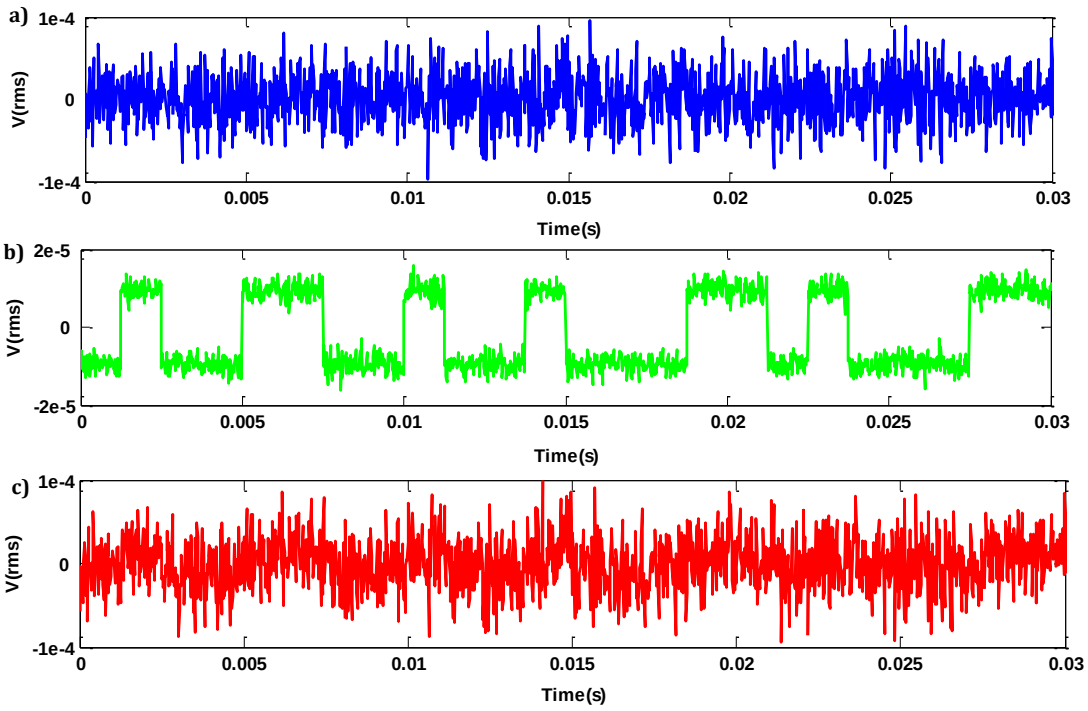

Figure 6.1: (a) Thermal noise (30µVrms) vs. time (b) Burst noise (10µVrms) vs. time (c) Burst (10µVrms) and Thermal noise (30µVrms) vs. time

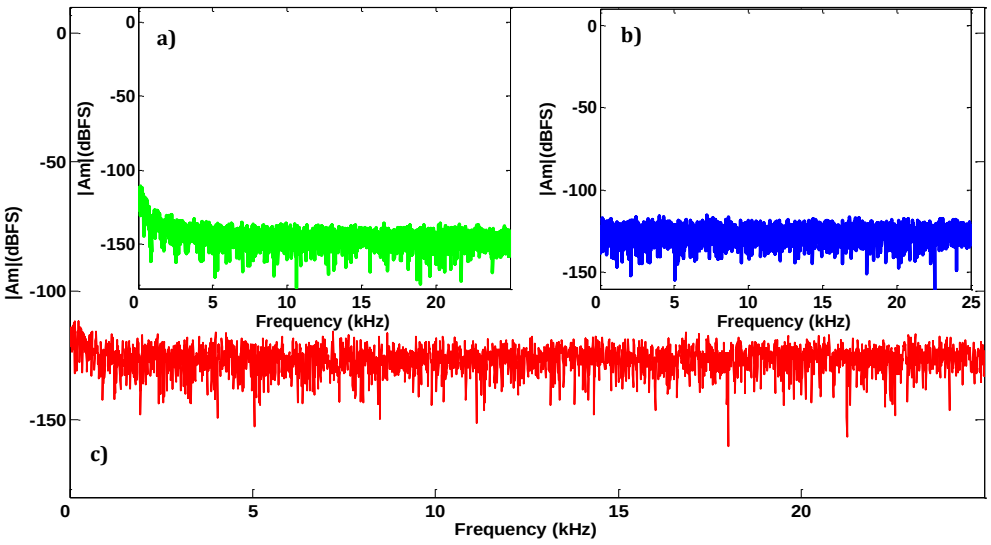

Figure 6.2: (a) Burst noise (30µVrms) vs. frequency. (b) Thermal noise (10µVrms) vs. frequency. (c) Burst (10µVrms) and Thermal noise (30µVrms) vs. frequency (1Vrms full-scale, f_S = 48 kHz)

6.2: RESULTS

The good and bad parts were simulated by varying the sample size (n) as well as the significance level (α) for a fixed bin size (k). In each instance the total number of parts that failed or passed the test were recorded in order to obtain the pass/fail percentages.

Good Parts Passed

The total good parts that pass the test are highlighted in Fig 6.3. The percentage of good parts that pass the test are invariant with changing sample sizes. It does however depend upon the statistical significance (α) as decreasing α values cause an increase in the percentage of good parts passed.

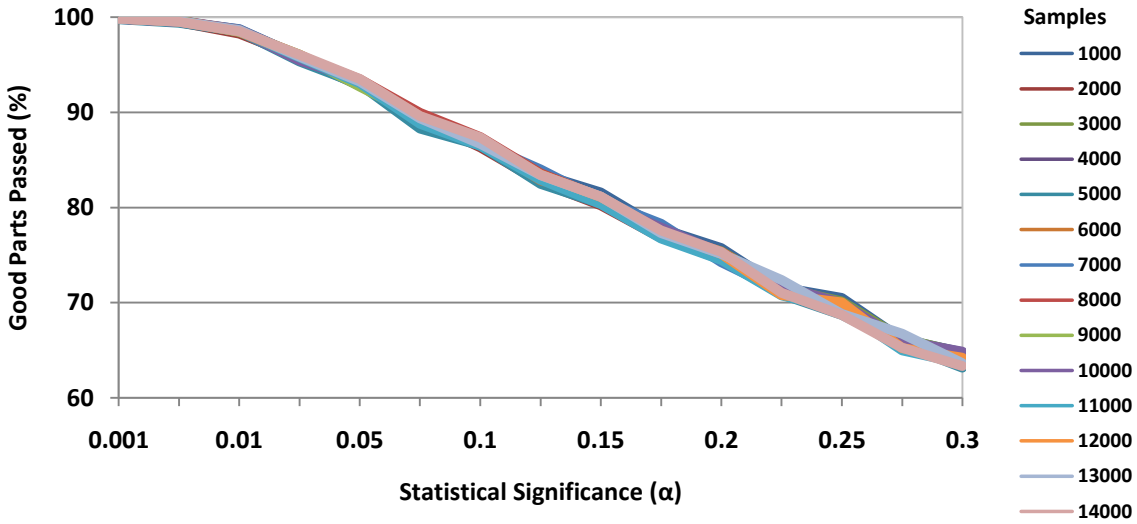

Figure 6.3: Good Parts Passed (%)

Theoretically α indicates the probability that a good part will fail the test. For example if α = 0.1, 90% of the good parts should pass the test. From the simulated

results, with α = 0.1, about 86% good parts pass the test. There is a good correlation between the simulated and theoretical probabilities with some error due to estimation.

Bad Parts Failed

Figure 6.4 highlights the total percentage of bad parts that fail the test. The total percentage of bad parts failed depends upon both the sample size (n) and the statistical significance (α). For a fixed α, the percentage of bad parts failed increases with increasing n, while for a fixed n, the percentage of bad parts failed increases with increasing α. This agrees with theory and highlights a tradeoff between the good parts passed and bad parts failed. Setting a higher α value would increase the percent of bad parts failed but would decrease the percent of good parts passed.

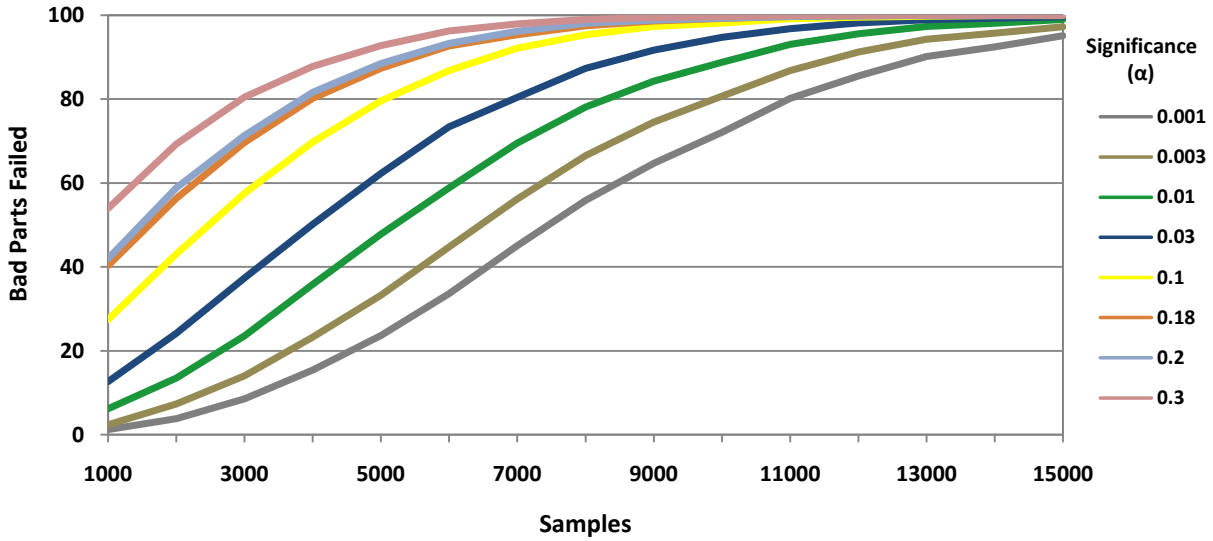

Figure 6.4: Bad Parts Failed (%)

6.3: SUMMARY

A primary goal of this study is to develop a test methodology which would fail 95% of the bad parts (which would be discarded in a real test environment) and pass 99%

of the good parts. The next chapter discusses a one pass (done for a single sample size) and a two pass (done with two different sample sizes) test with the use of the results obtained above.

Chapter 7: One/Two Pass Test

7.1: One Pass Test

A one pass test is constructed with a fixed sample size and statistical significance (α). All parts that pass the test are kept, while parts that fail are discarded. Using a sample size of 14000 samples and α = 0.003, 99% of the good parts pass and 95.5% of the bad parts fail the test. Figure 7.1 highlights the results obtained with a one pass run.

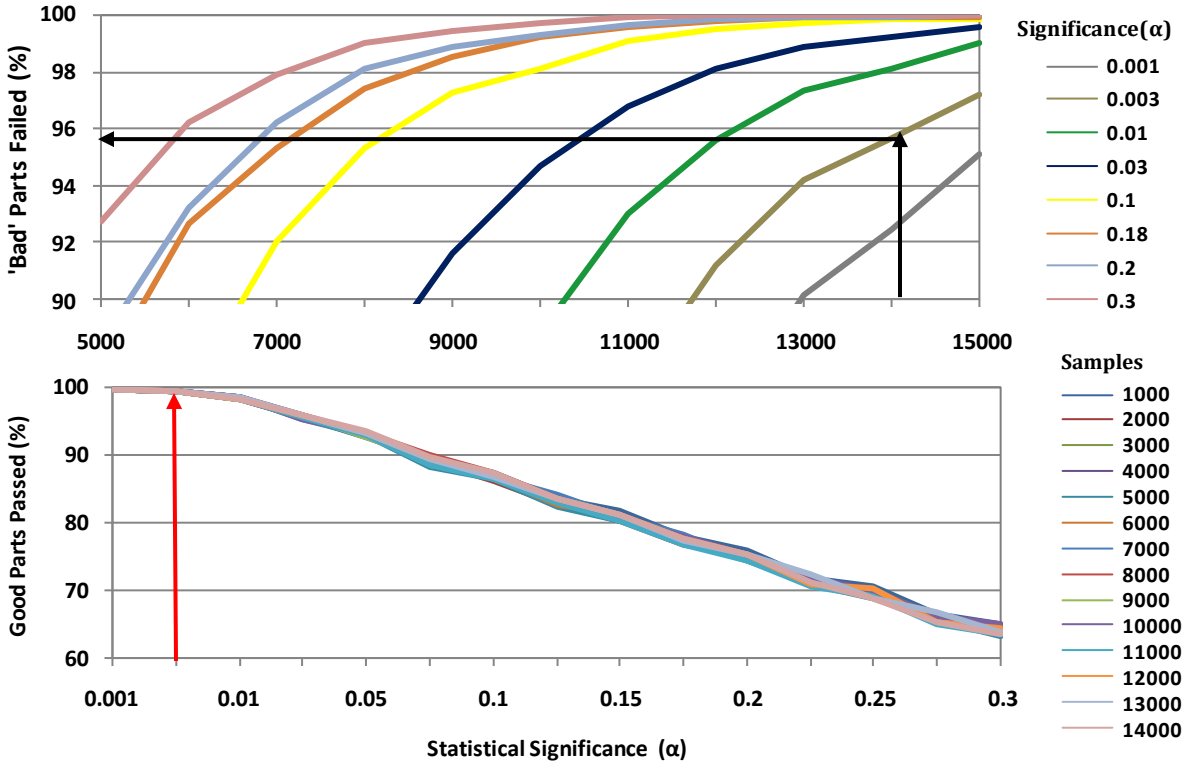

Figure 7.1: One Pass Test

7.2: TWO PASS TEST

The two pass test is executed using two samples sizes and significance levels (α). All parts are initially tested with sample size 1 (n_1) and α_1. Parts that pass the initial pass are kept as good while all parts that fail the initial pass are re-tested in a second pass with sample size 2 (n_2) and α_2. Parts that fail the second pass are discarded as bad while parts that pass are kept as good. Table 7.1 illustrates the truth table for the two pass test.

1st Pass	2nd Pass	Outcome
Pass	Part not re-tested	Part kept
Fail	Pass	Part kept
Fail	Fail	Part thrown away

Table 7.1: Two Pass Test Flow

Figure 7.2 illustrates a flowchart of the two pass test.

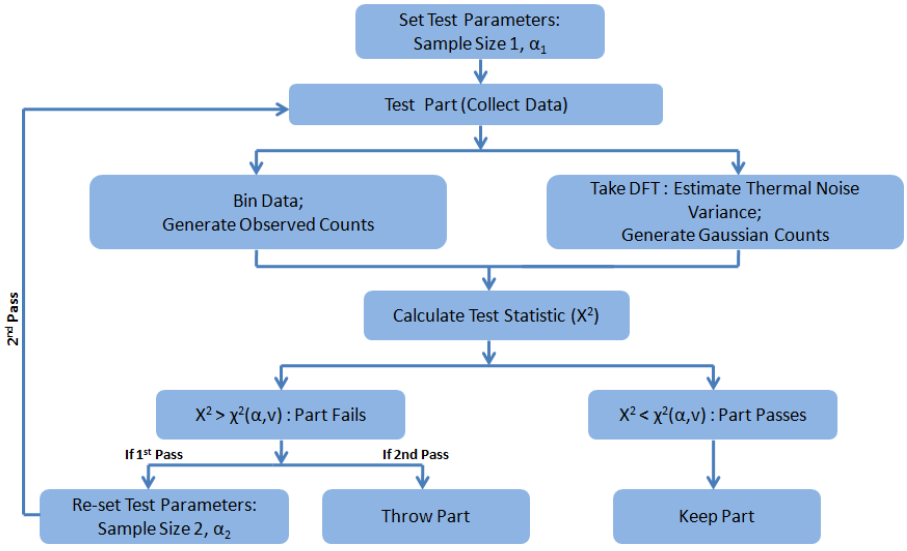

Figure 7.2: Flowchart of the Two Pass Test

As parts that fail the initial pass are not re-tested, the bad parts that slip through the initial pass are limited to less than 5%. The second pass is used to optimize the yield in order to pass 99% of all good parts.

The sample sizes (n_1 and n_2) and the significance levels for the two passes can be determined from the results discussed in Chapter 6. As an example Figure 7.3 highlights a possible solution.

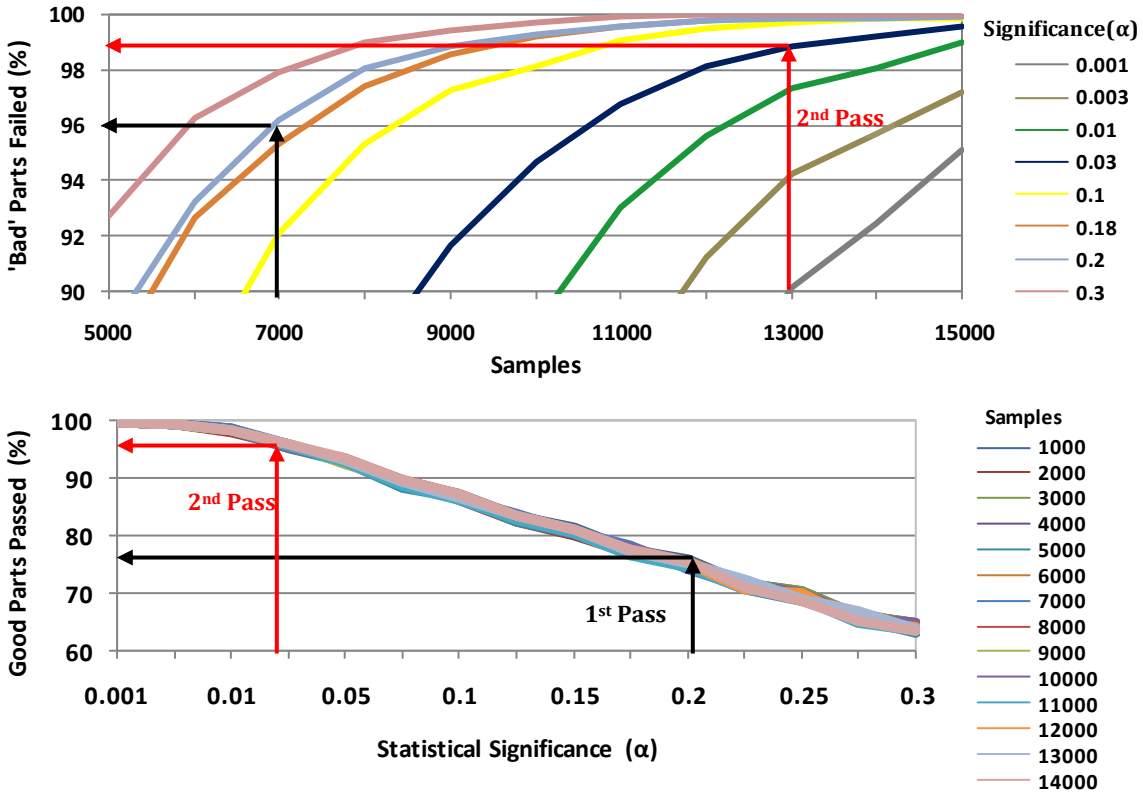

Figure 7.3: Two Pass Test

The first pass is run with 7000 samples (highlighted in Figure with black) and α of 0.2. With this test setup, 96% of the bad parts failed and 75% of the good parts passed in the 1st pass. In the 2nd pass, the 96% bad parts and 25% good parts that failed the 1st pass are re-tested with a 2nd pass sample size of 13000 samples and α of 0.03. 99% of the bad parts are failed and 96% of the good parts are passed in the 2nd Pass.

As the both passes are independent, the joint pass/fail probability of the two passes can be calculated as the product of the probabilities obtained from each pass. This results in a total of 99% good parts passed and 95% bad parts failed. Table 7.2 summarizes the results for the two pass test parameters discussed.

	1st Pass	2nd Pass	Total
Good Parts Passed	**75%** Re-test 25% →	**96%**	**75% + (25%*96%) = 99%**
Bad Parts Failed	**96%** Re-test 96% →	**99%**	**96%*99%=95%**

Table 7.2: Two Pass Test Results

7.3: TOTAL TEST TIME

The total test time was calculated by assuming a total population of 1 million parts with 8000 bad parts at a sampling rate of 48 kHz. The total test time was calculated using:

$$T = \frac{1}{f_S} * n * units \qquad 7.1$$

For a one pass test with 14000 samples, the total test time was 81 hours. While for a two pass test with 7000 samples the total test time was 48 hours. The two pass test time gives 40% reduction in test time with the same yield and bad parts detected.

7.4: OPTIMAL TWO PASS TEST

The two pass parameters discussed in the sections above is not the only solution required in order to pass a total of 99% good parts and fail 95% bad parts. The optimum solution can however be determined by analyzing the total test time required for all possible solutions. From fig 7.4, plotted for different two pass test parameters, it can be seen that the optimal solution in terms of the total test time is obtained using 1st pass with 7000 samples.

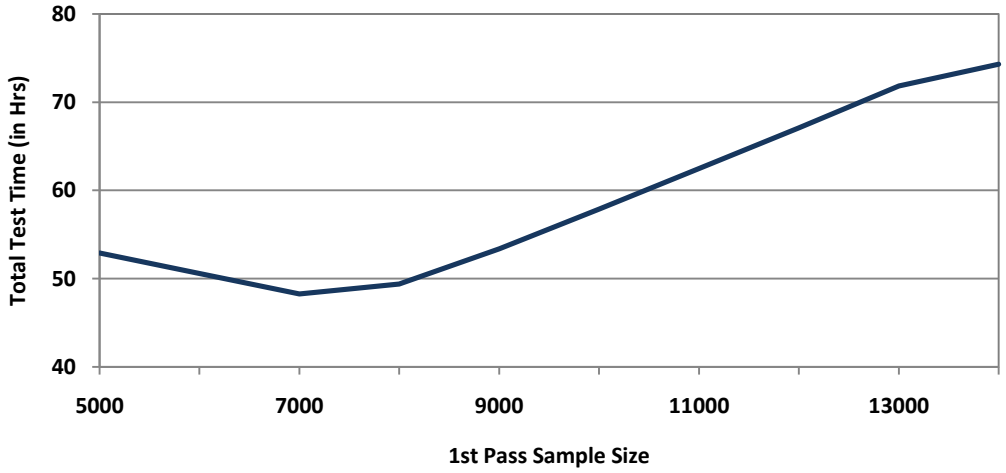

Figure 7.4: Total Test Time vs. 1st Pass Sample size

For sample sizes above and below 7000 samples the test time increases. As there is a tradeoff between the good parts that pass (which increases with decreasing α) and bad parts that fail (which increases with increasing α), the total test time for a two pass test with a $n_1 < 7000$ is dominated by the need to retest more good samples that fail the 1st pass. For $n_1 > 7000$, the total test time is dominated by the 1st pass sample size.

7.5: SUMMARY

The results obtained and test parameters used for the devised one and two pass test are summarized in Table 7.3 below.

Bins (k) = 20	**α**	**No of Samples**
One Pass Test	0.003	14000
Two Pass Test - 1st Pass - 2nd Pass	 0.2 0.03	 7000 13000

Table 7.3: Summary of Results

Chapter 8: Discussion

This study has so far highlighted the feasibility of the Goodness of Fit test in detecting burst noise in test chips.

The advantages of the use of the Goodness of Fit test include the detection of low levels of burst noise in test data. Standard test procedures currently implement a Discrete Fourier Transform of the data in order to test other performance parameters. Estimation of the thermal noise variance incorporated in the test procedure described in this study can thus be included easily in current test flows.

Several assumptions need to be addressed before this method is established. The Matlab models generated random statistically independent test data. Any non-independent samples could alter the statistics obtained in this study. The bin size for this study was set at 20 bins as increasing bin sizes limit the power of the test.

The power of the Chi-Squared Goodness of Fit is difficult to mathematically model. Power studies for the Chi-Squared Goodness of Fit test have been thus far been limited to simulation results [13] and an analytical model presented for the uniform distribution. As the test requires an established statistical significance (α) level for both the two pass and one pass test structures, the optimum α value needs to be predetermined by tests with actual test data. This value cannot be analytically or mathematically set as the α value is highly dependent on the power of the test.

ONE PASS VS. TWO PASS TEST STRUCTURE

As highlighted in Chapter 9, the two pass test structure provides an overall reduction in the total test time with the same yield and bad parts detected as compared to a one pass test. The current Two Pass structure requires re-measurement of the part in the 2^{nd} Pass with a higher sample size. Assuming in a two pass test, the 1^{st} pass is executed with 7000 samples and the 2^{nd} pass with 13000 samples, a proposed method to further reduce test time could be implemented during the actual testing of part. If a part fails the 1^{st} pass only 6000 more samples are re-measured. The initial 7000 sample data generated for the 1^{st} Pass would be used along with the newly generated 6000 sample test data to execute the 2^{nd} Pass. This could cause a small deviation from the current Two Pass results due to joint probability effects.

In order to successfully remove parts with burst noise from a set of units, a two pass test structure seems likely to be implemented. Further methodologies to devise a time efficient multi-pass test structure need to be investigated.

Appendix

Matlab Code: gof.m

```
% Shubra Marwaha : Goodness of Fit Test
% gof.m
% Files called: burst.m

%Test Parameters
num_bins = 20;
num_samp = 1000;
alpha = [0.0010   0.01 0.03 0.05 0.1      0.13 0.15 0.2];
hold_time = 60;
std_thermal = 30e-6;
std_burst = 10e-6;

count_fail = zeros(length(num_samp),length(alpha));
count_pass = zeros(length(num_samp),length(alpha));

    for m = 1:10000

    % Inputs
        vin1 = std_thermal.*randn(num_samp,1);
        vburst = burst(num_samp,hold_time,std_burst);

    %  Good Parts
        %  vin = vin1;

    %  Bad Parts
        vin = vin1 + vburst;

    % Mean of sampled data

        mean1 = sum(vin)/num_samp;
        mean_bins = mean1.*ones(num_bins-1,1);
        mean_num_samp = mean1.*ones(num_samp,1);

    % Variance of sampled data

        y = fft(vin);
        y_abs = abs(y);
        y_square = y_abs.*y_abs;

        %Addition of fs/4 bins through 3fs/4
        bin_fs4  = (num_samp/4);
        bin_3fs4 = (3*num_samp/4)-1;
        sum1 = 0;

        for i = bin_fs4:1:bin_3fs4
            sum1 = sum1 + y_square(i);
```

```
    end

    sum1 = 2*sum1;
    variance = sum1/(num_samp^2);
    std_dev = sqrt(variance);
    std_dev_bins = std_dev.*ones(num_bins-1,1);

%  Bins Intervals
    % Bin Intervals for a Standard Gaussian

    p = 1/num_bins;

    for i = 1:num_bins-1
        x(i)= norminv(p);
        p = p + 1/num_bins;
    end

    E(1) = normcdf(x(1));
    E(num_bins) = 1- normcdf(x(num_bins-1));

    for i = 1:num_bins-2
        E(i+1)= normcdf(x(i+1))- normcdf(x(i));
    end

    E = E.*num_samp;

    % Bin Intervals for a Gaussian with mean and std_dev estimated
    x = std_dev_bins'.*x + mean_bins';

% Observed Counts

    obs = zeros(num_bins,1);
    for j = 1:num_samp
        if(vin(j)< x(1))
            obs(1) = obs(1)+ 1;
        end

        if(vin(j)>x(num_bins-1))
            obs(num_bins) = obs(num_bins)+ 1;
        end
    end

    for i = 1:length(x)-1
        for j = 1:num_samp
            if(vin(j)>=x(i) & vin(j)<=x(i+1))
                obs(i+1) = obs(i+1) +1;
            end
        end
    end

% Chi Squared Statistic

    chi =  ((obs - E').^2)./E';
```

```
        chi = sum(chi);

    % Extra -2 in Degrees of Freedom to account for biased/estimated
variance
        dof = length(obs)-1-2;

    % Generating a Chi-squared statistic with significance level alpha
    % and degrees of freedom (dof)in-order to test generated chi
    % statistic.
    % If chi > chisquare_left test fails.

        for w = 1:length(alpha)

            alpha_tail = 1-alpha(w);
            chisquare_left = chi2inv(alpha_tail,dof);

            if chi>chisquare_left
                count_fail(1,w) = count_fail(1,w)+1;
            end

            if chi<chisquare_left
            count_pass(1,w) = count_pass(1,w) +1;
            end
        end
   end
```

Matlab Code : burst.m

```
function burst_wave = Burst(num_samp,hold_time,std_burst)

burst_wave = [];
thermal_rms = 0.3;

% Uniformly Distributed Random Numbers btwn -0.5 -> 0.5

t = -0.5 + rand(floor(num_samp/hold_time)+1,1);
rw = sign(t);

% Quantizing levels using the Signum function

for i = 1:floor(num_samp/hold_time)+1
     s = rw(i).*ones(hold_time,1);
     noise = thermal_rms*randn(hold_time,1);
     s = s + noise;
     burst_wave =[burst_wave;s(1:hold_time,1)];
end

%Scaling Burst Noise

burst_wave = burst_wave*std_burst;
burst_wave = burst_wave(1:num_samp,1);
```

References

[1] Buckingham, M. J., Noise in Electronic Devices and Systems. John Wiley & Sons, Inc, 1983.

[2] Operational Amplifier Noise Prediction, Intersil Application Notes, AN519.1, 1996.

[3] Doernberg, J.; Lee, H.-S.; Hodges, D.A., "Full-speed testing of A/D converters," *Solid-State Circuits, IEEE Journal of* , vol.19, no.6, pp. 820-827, Dec 1984.

[4] Lis,J. Noise Histrogram Analysis, Crystal Semiconductor Corp., Application Note AN37,1996.

[5] Montgomery, D. C. and Runger, G. C. Applied Statistics and Probability for Engineers. John Wiley & Sons,Inc, 4th Ed,2007.

[6] The MathWorks Web Page: http://www.mathworks.com/

[7] Oppenheim, A. V. and Schafer, R. W. Discrete-Time Signal Processing. Prentice Hall, Englewood Cliffs, NJ, 1989.

[8] Swanson, E., EE382M: Mixed Signal System Design and Modeling Austin course notes, The University of Texas at Austin, 2008.

[9] Van der Zeil, A. Noise in Solid State Devices and Circuits, Wiley-Interscience, 1986.

[10] D'Agostino, R. B. and Stephens, M. A. Goodness-Of-Fit Techniques. Marcel Dekker, Inc, vol.68, 1986.

[11] NIST/Sematech Engineering Statistics Handbook Webpage: http://www.itl.nist.gov/div898/handbook/

[12] Sturges (1926), H. A. "The choice of a class interval". *J. American Statistical Association*: 65–66

[13] Roscoe, J.T. and Bryars, J.A (1971). "An Investigation of the Restraints with Respect to the Sample Size Commonly Imposed on the Use of the Chi-Square Statistic", *J. American Statistical Association*: 755-759.

This document does not include the vita page from the original.